ELSEVIER
Available online at www.sciencedirect.com
ScienceDirect
Procedia Engineering 14 (2011) 336–343
Procedia Engineering
www.elsevier.com/locate/procedia

The Twelfth East Asia-Pacific Conference on Structural Engineering and Construction

NUMERICAL ANALYSIS OF CONCRETE MATERIAL PROPERTIES AT HIGH STRAIN RATE UNDER DIRECT TENSION

Y. F. HAO[a], X. H. ZHANG[a], and H. HAO[a]*

[a] *School of Civil and Resource Engineering, the University of Western Australia, Australia*

Abstract

The tensile strength of concrete material increases with the strain rate. Dynamic tensile strength of concrete material is usually obtained by conducting laboratory tests such as direct tensile test, flexural test, spall test or splitting test (Brazilian test). Some codes of practice such as Comite Euro-International du Beton (CEB) give empirical relations of concrete material dynamic increase factor (DIF) based on testing data. However, the reliability of the dynamic testing and the derived DIF are under debating. It is commonly agreed now that the DIF obtained from dynamic impact test is affected by lateral inertia confinement effect. Therefore, those derived from testing data do not truly reflect the dynamic material properties. The influence of the lateral inertia confinement, however, is not quantified. Moreover, concrete is a heterogeneous material with different components, but is conventionally assumed to be homogeneous, i.e. cement mortar only, in most previous experimental or numerical studies. In the present study, a mesoscale concrete material model consisting of cement mortar, aggregates and interfacial transition zone (ITZ) is developed to simulate direct tensile tests and to study the influences of the lateral inertia confinement and heterogeneity on tensile strength increment of concrete materials with respect to strain rates. The commercial software AUTODYN is used to perform the numerical simulations. The influence of lateral inertia confinement on tensile DIF of concrete material is examined.

Keywords: Concrete, high strain rate, mesoscale model, direct tension, ITZ, aggregate effect.

* Corresponding author and presenter: Email: hao@civil.uwa.edu.au

1877–7058 © 2011 Published by Elsevier Ltd. Open access under CC BY-NC-ND license.
doi:10.1016/j.proeng.2011.07.042

1. INTRODUCTION

Concrete is a common construction material used in both civil and defense engineering. For a better protection against high-rate loadings, e.g. impact or blast, and a more reliable design of concrete structures, it is important to understand the dynamic concrete material properties. The dynamic tensile strength of concrete is usually obtained by conducting laboratory tests such as direct tension test (Staab and Gilat 1991, Tedesco et al. 1991, Yan and Lin 2006), flexural test, spall test (Brara et al. 2001, Schuler et al. 2006) or Brazilian splitting test (Gomez et al. 2001). Although it is widely agreed that the tensile dynamic increase factor (DIF), defined as the ratio of dynamic to static strength, of concrete material increases with strain rate, a similar trend as its compressive DIF, apparent scatters from different tests can be observed (Malvar and Crawford 1998, Cotsovos and Pavlović 2008). These scatters can be attributed to variations in testing conditions such as apparatus, specimen material and specimen size. Besides these variations, it is known that inevitable lateral inertia confinement effect, which is specimen size dependent, also influences the testing results. Unfortunately, there is no systematic study yet on the influences of lateral inertia confinement on tensile DIF of concrete materials. Using the current empirical relations from the literature, which are derived mainly from testing data, would overestimate the concrete structural dynamic strength because the inertia confinement effect inevitably exists in dynamic testing. Moreover, real concrete consists of cement mortar, aggregate and interfacial transition zone (ITZ), but in most previous laboratory tests and numerical simulations, it is assumed as a homogeneous material with cement mortar only. Because different components in a concrete mix have different material properties, modelling concrete by cement mortar only results in inaccurate predictions of concrete material properties in both experimental and numerical studies. The present study develops mesoscale models of concrete specimens with consideration of cement mortar, aggregates and ITZ to investigate the influence of lateral inertia confinement on dynamic tensile strength of concrete specimens under direct tensile tests. The materials are assumed to be strain rate sensitive and insensitive, respectively, where DIF derived from strain rate sensitive materials is caused by a combination of strain rate effect and lateral inertia effect while DIF derived from strain rate insensitive materials is caused by only lateral inertia confinement. Because the lateral inertia confinement effect is specimen size dependent, the radius of the specimen varies from 6 mm to 50 mm in this study, thus allowing for a direct observation and quantitative assessment of the lateral inertia confinement effect contributions to the concrete tensile DIF.

2. MATERIAL MODEL

An accurate material model is essential for a reliable simulation of structural response and damage. The material model used in the present study includes equation of states (EOS), strength criterion, damage model and a model for strain rate effect, which is the same as in (Hao et al. 2010). It should be noted that the property of ITZ is not well understood yet, and it is assumed to be a weak mortar, with the same material model but has lower strength in the present study. A P-α EOS is employed for mortar and ITZ whereas a linear EOS is used for aggregates. A piecewise Drucker-Prager model and Mazars' damage model are used for all three components. The tensile DIF relations defined below are used for strain rate sensitive cement mortar and ITZ (Hao and Zhou 2007)

$$TDIF = 1.0 \qquad \text{for} \quad \dot{\varepsilon} \le 10^{-4} s^{-1} \tag{1}$$

$$TDIF = 0.26 \log \dot{\varepsilon} + 2.06 \qquad \text{for} \quad 10^{-4} s^{-1} \le \dot{\varepsilon} \le 1 s^{-1} \tag{2}$$

$$TDIF = 2 \log \dot{\varepsilon} + 2.06 \qquad \text{for} \quad \dot{\varepsilon} > 1 s^{-1} \tag{3}$$

while those for aggregate are (Zhou and Hao 2008).

$$TDIF = 0.0225 \log \dot{\varepsilon} + 1.12 \qquad \text{for} \quad \dot{\varepsilon} \leq 0.1 s^{-1} \tag{4}$$

$$TDIF = 0.7325 (\log \dot{\varepsilon})^2 + 1.235 (\log \dot{\varepsilon}) + 1.6 \qquad \text{for} \quad 0.1 s^{-1} \leq \dot{\varepsilon} \leq 50 s^{-1} \tag{5}$$

The material parameters are listed in table 1.

Table 1: Material parameters

	Mortar	ITZ
Initial density (kg/m3)	2.405×103	1.8×103
Solid density (kg/m3)	2.75×103	2.75×103
Initial soundspeed (m/s)	2.97×103	2.269×103
Initial compaction pressure (MPa)	36	16.2
Solid compaction pressure (MPa)	6×103	6×103
Solid bulk modulus (GPa)	35.27	35.27
Damage parameters	0.5	0.5
Compressive damage threshold	2×10-3	2×10-3
Tensile damage threshold	2×10-4	2×10-4
Compressive strength (MPa)	57.7	23
Tnesile strength (MPa)	4.53	1.8
Cut-off tensile strength (MPa)	2.5	0.9

Aggregate	
Density (kg/m3)	2.75×103
Bulk modulus (GPa)	35.7
Shear modulus (GPa)	17.44
Damage parameters	0.5
Compressive damage threshold	3.6×10-3
Tensile damage threshold	3.6×10-4
Compressive strength (MPa)	200
Tnesile strength (MPa)	15
Cut-off tensile strength (MPa)	7.5

3. SHPB SIMULATION AND SIMPLIFIED MODEL VERIFICATION

To calibrate the numerical model, it is used to simulate an SHPB test reported in (Tedesco et al. 1991). Figure 1 shows the axis-symmetrical model for the SHPB test. The specimen with notch made of mortar only is sandwiched between the two pressure bars. The geometry, stress boundary and material parameters are the same as those in (Tedesco et al. 1991), in which the specimen dimension is 50.8×50.8 mm (length × diameter) with a 3.175 mm square notch at mid-length. The incident bar and transmitter bar are respectively 3350×50.8 mm and 3660×50.8 mm. Gauges are attached at the centres of the pressure bars. Another nine gauges, with three at each interface between specimen and two pressure bars and at the notch are attached on the specimen. The stress-time history recorded in the pressure bars from the present simulation is shown in figure 2 and the reading from the experimental study is shown in figure 3. As shown, the numerical simulation closely reproduces the recorded stress waves in the incident and transmitter bar from the experimental study, indicating the reliability of numerical simulations of SHPB tests.

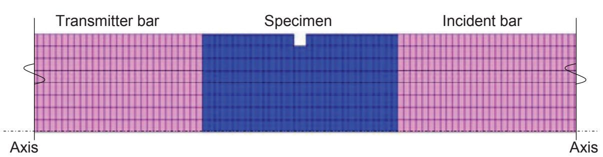

Figure 1: Numerical model of the SHPB test

Above simulation is very time consuming. In a previous study of compression SHPB tests of concrete specimens, it was found that replacing the pressure bars with proper velocity boundaries, i.e., only the specimen is included in the model, substantially reduced the computational time while yielded reliable simulations of the SHPB test (Hao et al. 2010). To verify the applicability of this approach to simulate SHPB tensile tests, a model with only the concrete specimen is developed. One end of the specimen is fixed and a trapezoid velocity boundary is applied to the other end. In the test by Tedesco et al. (1991), the strain rate is 4.9/s. Since the length of the specimen is 50.8 mm, to obtain the approximate uniform strain rate of 4.9/s in the specimen, the tensile velocity applied to the specimen is 0.25 m/s. The velocity boundary applied to the specimen has the same shape as in in the test shown in Figure 3 (Tedesco et al. 1991). It increases quickly from zero to 0.25 m/s with a rising time of 45 μs, and remains as a constant at this value for 100 μs , and then drops to zero in 45 μs. Very similar simulation results of the stress and strain in the specimen from this simplified model and the detailed model with both bars are observed. Table 2 compares the simulated peak stresses in the specimen from the two approaches. it is clear that the simplified numerical model is reliable to simulate SHPB tensile tests. Since the simplified model requires substantially less computer memory and less simulation time, it is used in the present study.

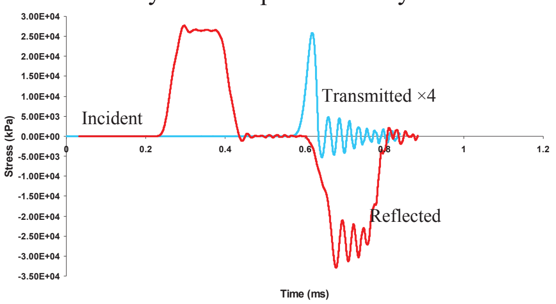

Figure 2: Simulation of incident, reflected and transmitted stress wave in SHPB test in the present study

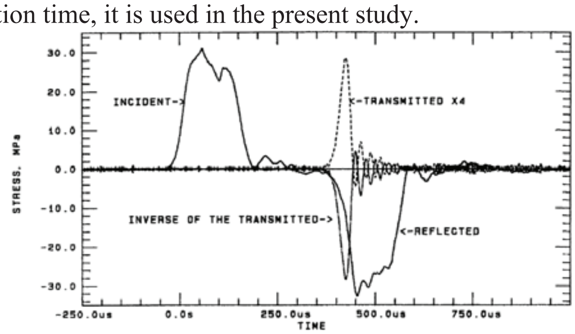

Figure 3: Experimental results of incident, reflected and transmitted stress for case 1 (Tedesco et al. 1991)

Table 2: Comparison between simplified and complete SHPB simulations

	Middle layer (3 gauges)	Side layers (6 gauges)	All (9 gauges)
Difference of average peak stress	4.3%	1.21%	2.5%

4. MESOSCALE NUMERICAL MODEL

Axis-symmetrical numerical model is adopted to simulate the cylindrical specimen. Proper attentions are paid to estimate the aggregates distributions in this axis-symmetrical model. To simplify the modelling process, aggregates are assumed to have circular cross sections. The geometry of the circular aggregates is approximately modelled by the square elements.

Since the thickness of ITZ ranges from 10 to 50 μm, modeling ITZ requires a finer element mesh and more computational memory. Moreover, the dynamic material properties of ITZ are poorly understood. To investigate the influence of ITZ on concrete DIF, a 6×12 mm specimen is chosen for preliminary numerical simulation using strain rate sensitive materials. Two models as shown in figure 4 are developed. The only difference in these two models is that one includes ITZ and the other one ignores ITZ between cement mortar and aggregates. The thickness of ITZ is assumed to be 50 μm. It should be noted that because there is no dynamic material properties of ITZ are available, in the present study, mortar material model with lower strength is used to model ITZ. The tensile strength of mortar is 4.53 MPa and that of ITZ is assumed to be1.8 MPa. The tensile DIFs derived from those two models with respect to strain rate are plotted in figure 5. As shown, the two models with or without considering ITZ in the model give very close simulation results. This is because DIF is a ratio of dynamic to static strength. The effect of ITZ in the model is normalized when calculating DIF. This observation indicates that if only DIF is of concern, ITZ can be neglected in the numerical simulations. In the subsequent simulations, ITZ is not considered in the model to reduce the simulation time.

The DIF of cement mortar is also plotted in the Figure. As shown, the simulated DIF in this study is slightly larger than that of cement mortar. This is due to the aggregates inside the specimen because aggregate has higher tensile strength compared to the other two components of concrete, indicating the importance of considering aggregates in the study.

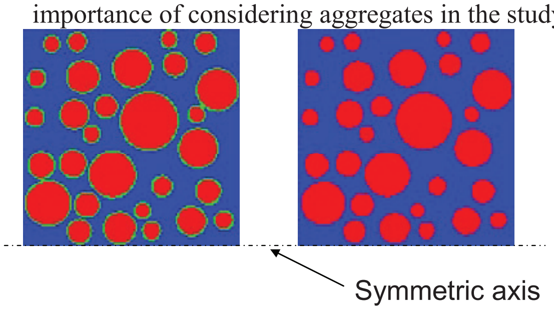

Figure 4: 6×12 mm specimens with and without ITZ

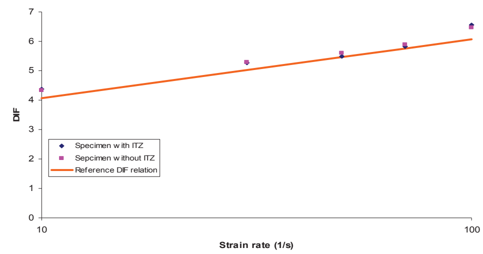

Figure 5: Comparison of DIFs from specimens with and without ITZ

Four series of specimen with increasing dimensions, i.e.. 6×12mm, 10×20mm, 20×40 mm and 50×100mm, are simulated with strain rate varying from 1/s to 150/s. Because the lateral inertia confinement effect on concrete DIF is size-dependent (Hao et al. 2010), increasing the specimen diameter allows a direct observation and a quantitative assessment of the lateral inertia confinement effect. Each specimen is designed to contain 40% aggregates. After the generation of the aggregates with random diameter and random position, the axis-symmetrical mesoscale numerical models of specimens are plotted in figure 6 where the blue part is the cement mortar and red circles denote aggregates in the specimen.

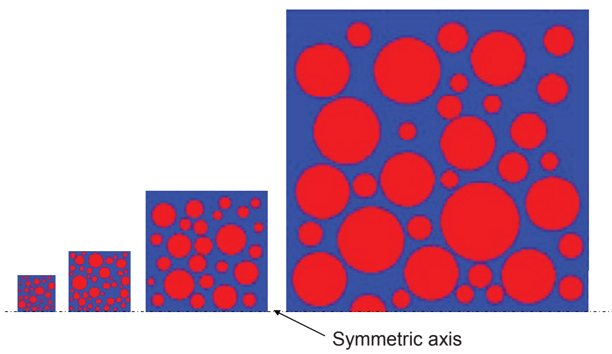

Figure 6: Mesoscale numerical model with 40% aggregates

5. NUMERICAL RESULTS AND DISCUSSION

Specimens with varying diameters, e.g. 12 mm to 100 mm, are simulated with respect to strain rates from 1 to 150/s using the strain rate sensitive and insensitive material models. It is assumed that DIFs obtained from the strain rate sensitive materials are caused by the combinations of strain rate effect and lateral inertia confinement effect whereas DIFs from strain rate insensitive materials are only caused by lateral inertia confinement effect. DIFs obtained from strain rate insensitive materials are plotted in figure 7 where 6_12mm corresponds to the 6×12mm specimen. It is clear that the lateral inertia confinement does contribute to the DIF in dynamic tension, and the lateral inertia confinement effect is strain rate effect, i.e. DIF increases with strain rate. It is also found that increasing the specimen size leads to larger DIFs at a certain strain rate, indicating that the lateral inertia effect is specimen size dependent.

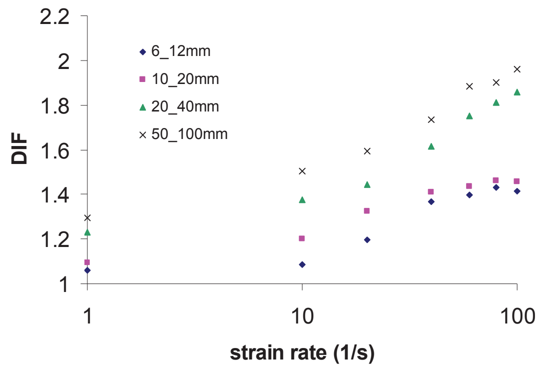

Figure 7: DIFs obtained from strain rate insensitive materials

DIFs obtained from the strain rate sensitive materials are plotted in figure 8. The reference DIF relation, which is used to define material DIFs in the simulations, is also plotted in the figure for comparison purpose. It can be seen that all data are higher than the reference DIF curve. This can be attributed to the lateral inertia confinement effect, and the aggregates effect. The reference DIF is commonly used to define concrete DIF. They were obtained from laboratory tests of concrete specimens. In those tests, the lateral inertia confinement effect always exists. Direct use of these testing data results in a double account of the lateral inertia confinement effect, leading to overestimations of the DIF. On the other hand, owing to the restrictions in performing high-speed impact tests, in most tests, only cement mortar was used to prepare the concrete specimens. Since aggregates has higher tensile strength, without aggregates in the specimen might result in underestimation of concrete strength. As explained in reference (Hao et al. 2010), when the strain rate is low, the stress wave can seek weaker sections, e.g. cement mortar, to propagate. However when the strain rate is high, the stress wave has no time to seek weaker sections but has to propagate through aggregate, resulting in higher dynamic tensile strength and DIF. These observations indicate that direct use of the DIF from laboratory tests might not necessarily lead to an accurate prediction of concrete material DIF.

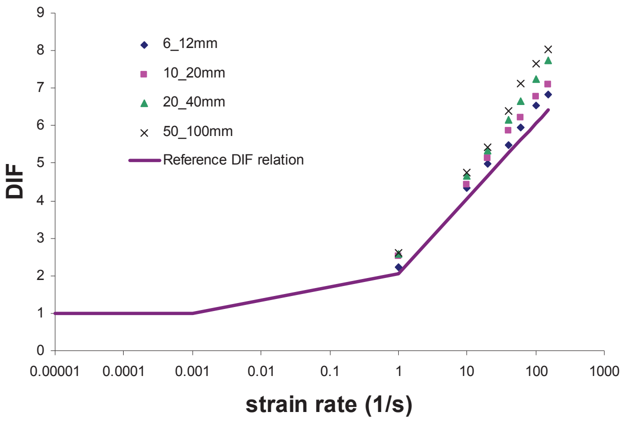

Figure 8: DIFs obtained from strain rate sensitive materials

To quantify the relative contributions of the lateral inertia confinement in mesoscale concrete model of different specimen sizes to DIF, the ratios of the corresponding DIFs obtained with strain rate insensitive materials to those with strain rate sensitive materials are shown in figure 9. As shown again the lateral inertia confinement effect is specimen size dependent and increases with the strain rate. It is interesting to note that increasing the specimen diameter from 12mm to 20mm, then from 20mm to 40mm, the contribution from lateral inertia confinement increases almost linearly with the increase of specimen diameter. However when increasing the diameter from 40mm to 100mm, the increase of lateral inertia confinement effect is no longer linear.

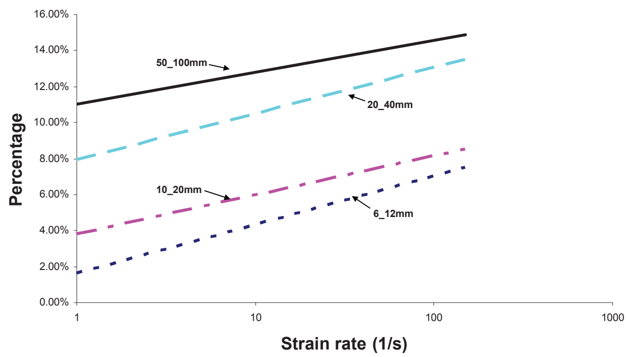

Figure 9: Lateral inertia contribution to DIF

6. CONCLUSION

This paper presented numerical simulation results of SHPB tests of concrete specimens under direct tension to study concrete tensile DIF. Numerical results indicate that the concrete material strength increment with strain rate is caused by a combination of strain rate effect (material property) and lateral inertia confinement effect (structural response). The lateral inertia confinement effect increases with the strain rate and the specimen size. The results demonstrate the effect of lateral inertia confinement in high-speed impact tests of material properties, and the importance of including aggregates in experimental tests and numerical simulations of dynamic concrete material properties. The inevitable lateral inertia confinement effect in dynamic tests results in an overestimation of concrete DIF, whereas using cement mortar only to prepare concrete specimen without aggregates may underestimate the DIF of concrete at high strain rates. Therefore it should be cautions when using DIF obtained from dynamic impact tests. The reliability of using numerical simulations of SHPB test is demonstrated.

ACKNOWLEDGMENTS

The authors would like to thank Australian Research Council for financial support under grant No. DP1096439. The first author also acknowledges the SIRF scholarship from the University of Western Australia.

REFERENCES

[1] Brara A, Camborde F, Klepaczko JR and Mariotti C (2001). Experimental and numerical study of concrete at high strain rates in tension. Mechanics of Materials, 33(2001), pp. 33-45.

[2] Cotsovos DM and Pavlović MN (2008). Numerical investigation of concrete subjected to high rates of uniaxial tensile loading. International Journal of Impact Engineering, 35(2008), pp. 319-335.

[3] Gomez JT, Shukla A and Sharma A (2001). Static and dynamic behavior of concrete and granite in tension with damage. Theoretical and Applied Fracture Mechanics, 36(2001), pp. 37-49.

[4] Hao H and Zhou XQ (2007). Concrete material model for high rate dynamic analysis. Proceedings Seventh International Conference on SHOCK & IMPACT LOADS ON STRUCTURES, Beijing, pp. 753-768.

[5] Hao YF, Hao H, and Li ZX (2010). Numerical analysis of lateral inertial confinement effects on impact test of concrete compressive material properties. International Journal of Protective Structures, 1(1), pp. 145-167.

[6] Malvar LJ and Crawford JE (1998). Dynamic increase factors for concrete. Proceedings Twenty-Eighth DDESB Seminar, Orlando, FL.

[7] Schuler H, Mayrhofer C and Thoma K (2006). Spall experiments for the measurement of the tensile strength and fracture energy of concrete at high strain rates. International Journal of Impact Engineering, 32(2006), pp. 1635-1650.

[8] Staab GH and Gilat A (1991). A direct-tension split Hopkinson Bar for high strain-rate testing. Experimental Mechanics, September, 1991, pp. 232-235.

[9] Tedesco JW, Ross CA, McGill PB, and O'Neil BP (1991). Numerical analysis of high strain rate concrete direct tension tests. Computers and Structures, 40(2), pp. 313-327.

[10] Yan DM and Lin G (2006). Dynamic properties of concrete in dynamic tension. Cement and concrete research, 36(2006), pp. 1371-1378.

[11] Zhou XQ and Hao H (2008). Modelling of compressive behaviour of concrete-like materials at high strain rate. International Journal of Solids and Structures. 45, pp. 4648-4661.